Title

Enhanced axonal transport: A novel form of “plasticity” after primate and rodent spinal cord injury

Journal

Experimental Neurology, 301(Pt A)

ISSN

0014-4886

Authors

Brock, JH

Rosenzweig, ES

Yang, H

et al.

Publication Date

2018-03-01

DOI

10.1016/j.expneurol.2017.12.009

Peer reviewed

Published in final edited form as:

Exp Neurol. 2018 March ; 301(Pt A): 59–69. doi:10.1016/j.expneurol.2017.12.009.

Enhanced axonal transport: A novel form of "plasticity" after primate and rodent spinal cord injury

J.H. Brock[a,b], **E.S. Rosenzweig**[b], **H. Yang**[b], **M.H. Tuszynski**[a,b,*]

[a]Veterans Administration Medical Center, La Jolla, CA, United States

[b]Dept. of Neurosciences, University of California, San Diego, La Jolla, CA, United States

Abstract

Deficient axonal transport after injury is believed to contribute to the failure of CNS regeneration. To better elucidate neural mechanisms associated with CNS responses to injury, we transected the dominant voluntary motor system, the corticospinal tract (CST), in the dorsolateral T10 spinal cord of rhesus monkeys. Three months later, a 4.5-fold increase in the number of CST axons located in the spared ventral corticospinal tract at both the lesion site and, surprisingly, remotely in the *cervical* spinal cord was observed. Additional studies of increases in corticospinal axon numbers in rat and primate models demonstrated that increases were transient and attributable to enhanced axonal transport rather than axonal sprouting. Accordingly, increases in axonal transport occur after CNS injury even in the longest projecting pathways of the non-human primate, likely representing an attempted adaptive response to injury as observed in the PNS.

Keywords

Spinal cord injury; Non-human primate; Axonal transport

1. Introduction

Recent advances in spinal cord injury (SCI) research have revealed mechanisms that limit CNS plasticity and regeneration, and several experimental approaches for enhancing axonal growth after injury have been reported. Most of these advances utilize methods of axonal tract tracing to reveal the effects of experimental manipulations. The most common method of axonal labeling injects anterogradely transported tracers, including dextran-containing particles. Other studies use retrograde tracer injections within or below zones of injury to quantify the number of retrogradely labeled neurons in regions remote from the lesion site that have presumably extended axons that take up and transport the tracer. All of these methods depend on axonal transport for visualization of the experimental response.

Both anterograde and retrograde axonal transport are critical processes for sustaining neuronal function. Anterograde transport is mediated by kinesin motor proteins, while retrograde transport requires dynein proteins (Black and Lasek, 1980; Galbraith and Gallant,

*Corresponding author at: Dept. Neurosciences, 0626, University of California – San Diego, La Jolla, CA 92093, United States. mtuszynski@ucsd.edu (M.H. Tuszynski).

2000; McEwen and Grafstein, 1968; Scheff et al., 2003). Fast anterograde transport occurs at a rate of 50–400 mm/day, and slow anterograde transport occurs at two rates: 1) component “a” rate of 0.25 mm/day, which transports tubulin and neurofilament proteins, and 2) component “b” rate of 2–3 mm/day, which transports a variety of proteins including, actin (Black and Lasek, 1980; Galbraith and Gallant, 2000; McEwen and Grafstein, 1968; Scheff et al., 2003). Similar mechanisms have been identified that regulate retrograde axonal transport.

It has been known for some time that injury can influence axonal transport. Grafstein and Murray reported in the 1960s that optic nerve crush causes an increase in slow component b, based on transport of radiolabeled amino acids (Grafstein, 1969; Grafstein and Murray, 1969). More recent studies confirm alterations in axonal transport that may serve the purpose of carrying and organizing structural proteins required for formation of growth cone-like structures (Konzack et al., 2007; Mar et al., 2014a; Mar et al., 2014b). However, effects of lesions on axonal transport have been less thoroughly studied in the brain and spinal cord; indeed, it has been conjectured that a lack of increased axonal transport after central lesions may contribute to the failure of central axonal regeneration (Forbes and Andrews, 2017).

In the present experiment, we examined whether axons of the ventral corticospinal tract in rhesus monkeys undergo compensatory collateral sprouting after lesions of the majority (90%) component of the dorsolateral corticospinal projection. Ventral CST sprouting occurs in rodent models and is associated with partial improvement in motor function (Bareyre et al., 2004; Steward et al., 2008; Weidner et al., 2001), representing a form of endogenous axonal structural plasticity that may be associated with partial functional recovery. Given the dominance of corticospinal systems in primate motor control, we sought to characterize responses of the ventral CST after dorsolateral injury in rhesus monkeys. Subjects underwent lateral corticospinal tract lesions at T10, and the corticospinal tract was anterogradely traced during the same surgical session. Surprisingly, we observed a 4.5-fold increase in the number of CST axons in the ventral white matter not only at spinal cord levels caudal to the injury, but at remote cervical levels also. To confirm whether new axonal growth in host white matter actually accounted for this observation, we explored the alternative possibility that spared axons enhanced their uptake or transport of the biotinylated dextran-based tracer. Indeed, detailed examination of the timing, nature and rate of tracer transport indicated that alterations in tracer transport, rather than true new growth, accounted for our observations of increased numbers of axons in the lesioned primate and rodent spinal cord. These findings reveal the presence of metabolic “plasticity” of neuronal transport in the rodent and primate CNS that may prime the neuron for a reparative response, even if subsequent regeneration fails.

2. Materials and methods

2.1. Experimental design

This experiment was originally designed to examine the nature of spontaneous axonal adaptation to unilateral transection of the dorsolateral component of the primate corticospinal projection at the T10 level. Following initial findings in the primate model,

additional studies were performed in rodents to gain insight into mechanisms underlying observations in the primate model. Primate methods will be described first, followed by rodent methods.

For primate studies, the following groups were examined: Group 1 (Intact, N = 4) consisted of intact animals without spinal cord lesions that underwent tracing of the corticospinal tract (CST), with quantification of axons at the L4 spinal cord segment. Tracing time was sufficient (3 months) to allow the tracer to reach the lumbar spinal cord segment (Lacroix et al., 2004). Group 2 (Lesion/No Delay Trace, N = 5) consisted of animals that underwent T10 right dorsolateral CST transections. This lesion removes 90% of all CST axons originating from the left motor cortex that project down the right side of the spinal cord, together with 8% of CST axons originating from the right motor cortex that descend ipsilaterally down the spinal cord in the dorsolateral tract (Lacroix et al., 2004). Lesions spared the *ventral* CST on the right side, which contains 2% of CST projections that originate from the right motor cortex and travel down the spinal cord (Lacroix et al., 2004). CST axons were quantified at the L4 segment to assess responses of the spared right ventral CST after removal of the right dorsolateral CST. Tracers were injected during the same surgical session that CST lesions were placed. Group 3 (Intact Cervical, N = 3) consisted of intact animals that underwent tracing of the CST, with quantification of axons at the C8 spinal cord segment. Tracing time was sufficient (6 weeks) to allow the tracer to reach the cervical spinal cord segment; tracing times longer than 6 weeks result in movement of most tracer down the spinal cord, away from the mid-cervical segment. Group 4 (Lesion/Delayed Trace, N = 2) consisted of animals with right C7 dorsolateral CST transections that underwent tracer injections six weeks *after* spinal cord lesions were placed. Axons were quantified at the C8 spinal cord segment to assess responses of spared right ventral CST axons to removal of the dorsolateral CST. While we would have preferred to study a complete set of animals with lesions at a single spinal level (either all T10 or all C7), the lesion model was moved from T10 to C7 during the course of this primate research program to enable study of hand function in other experiments; we did not feel justified in subjecting additional monkeys to T10 lesion to address this specific experimental transport question. Instead, we opted to use data from right C7 dorsolateral quadrant lesions in monkeys and to perform additional studies in rat models to confirm findings form the primate model and gain insight into underlying mechanism, as described below. The monkey experiment design is summarized in Fig. 1 and the rat in Fig. 5.

2.1.1. Subjects—Fourteen adult male monkeys (*Macaca mulatta*; mean age 9.1 ± 5.3 years, range: 3.8–14.5 years) were studied. All surgical procedures were carried out using principles of the Laboratory Animal Care Act (National Institutes of Health Publication 85-23, revised 1985) and were approved by the Institutional Animal Care and Use Committee (IACUC).

2.1.2. Spinal cord lesions—Monkeys were housed individually. Induction of anesthesia was performed with ketamine HC1 (10 mg/kg i.m.) followed by maintenance with isoflurane. To create CST lesions, the level for laminectomy was identified by palpating rostrally from the T2 (C7 spinal level lesion) or T12 (T10 spinal level lesion) spinous

processes. A dorsal skin incision was placed over the identified C7 or T10 region and a dorsal laminectomy was performed. To place T10 spinal cord dorsolateral CST lesions, a microwire lesion knife (Kopf, General Valve, Fairfield, NJ) was positioned 0.5 mm lateral to the spinal cord midline on the right side, and lowered to a depth of 2 mm into the cord through a small dural incision. The wire knife was then extruded toward the right lateral aspect of the spinal cord, creating a final lesion dimension of 3 mm depth × 3 mm width (Fig. 1B). The wire was raised through the cord with the arc extended. Downward pressure was applied to the arc using a suction tip, thereby transecting all structures within the arc. Muscle and skin layers were sutured in layers. Post-operatively, the monkeys were provided analgesics routinely for 3–5 days and antibiotics for 5–7 days. All subjects retained bowel and bladder function following the lesion. This right-sided T10 spinal cord lesion transects approximately 90% of CST axons originating from the left motor cortex and 8% of CST axons originating from the right cortex (Fig. 1A) (Lacroix et al., 2004; Rosenzweig et al., 2009), but spares ventral CST axons on the right side of the spinal cord that originate from the right motor cortex. Nissl stained sections indicate that the lesion is contained entirely within the dorsal quadrant, sparing the ventral funiculus (Fig. 1). C7 cervical lesions were placed identically on the right side of the spinal cord in two monkeys, but at the C7 rather than T10 level (Rosenzweig et al., 2010).

2.1.3. CST tract tracing—Immediately or 2 months later, the corticospinal tract was anterogradely labeled as described previously (Lacroix et al., 2004; Rosenzweig et al., 2009; Rosenzweig et al., 2010). Biotinylated dextran amine (BDA; 10% in NaCl; 10,000 molecular weight, Molecular Probes, Eugene, OR) was injected into the right hemisphere to examine compensatory axonal responses to injury arising from neuronal cell bodies of the motor cortex primarily unaffected by the right-sided spinal cord lesion. 150 nl of the 10% BDA solution was injected at each site through a glass micropipette attached to a picospritzer. The medial/caudal boundary of the primary motor cortex was identified as the junction of the central sulcus with the inter-hemispheric fissure. The first tracer injection was placed 1 mm lateral to midline and 1 mm rostral to the central sulcus at 3 separate dorsal/ventral coordinates. The injections then proceeded linearly every 1 mm over 13 additional sites rostral to the central sulcus. Then a second and third row of injections were performed, each 1 mm lateral to each other. Three separate dorsal/ventral injections were made, which resulted in a total of 127 injection sites. These injection sites included areas of the motor cortex that innervate hand, trunk and foot areas. Each injection was made under microscopic guidance. Subjects survived an additional 6 weeks for cervical lesions or 3 months for thoracic lesions, to allow sufficient time for transport of BDA past the lesion into the cervical or lumbar enlargements, respectively (Lacroix et al., 2004; Rosenzweig et al., 2009; Rosenzweig et al., 2010).

2.1.4. Tissue processing and histology—Prior to perfusion, monkeys were sedated with ketamine (25 mg/kg; IM) and deeply anesthetized with Nembutal (30 mg/kg; IP). Subjects were perfused transcardially for 1 h with a 4% solution of paraformaldehyde in 0.1 M phosphate buffer (pH 7.4) at 4C followed by 5% sucrose solution. Spinal cords were removed and placed in a glycerin cryoprotectant solution. For detection of BDA labeling, spinal cords were sectioned on a cryostat set at 40 μm intervals. Sections were washed in

tris-buffered saline, pH 7.2 (TBS) and quenched in 0.6% H_2O_2 in TBS for 30 min. Following TBS washes, sections were incubated in ABC Elite reagent (1:100, Vector Laboratories, CA) in TBS + 0.25% triton-x overnight at 4 °C. Following TBS washes, sections were reacted with 1.25 mg/ml DAB, 0.04% $NiCl_2$, 0.012% H_2O_2 in TBS. Sections were then washed in TBS, mounted on gelatin-subbed slides, air dried, dehydrated and coverslipped with Entellan (Fisher Scientific, Pittsburgh, PA).

2.1.5. CST axon quantification—BDA-labeled axons were quantified within the contralateral dorsolateral tract (contralateral to the spinal cord lesion) using a stereological procedure, as described previously (Rosenzweig et al., 2009). Briefly, quantification was performed on an Olympus BX60 microscope equipped with an Olympus OLY-200 video camera, a motorized stage (MAC2002-XYZ, Ludl Electronic Products, Hawthorn, NY) and Stereo-Investigator software (MicroBrightField, Colchester, VT). A 60 × objective was used to count axons at 30–40 sampling sites (identified below) within a 50 × 50 μm square counting frame. To be counted an axon had to: 1) be clearly labeled; 2) pass through the plane of section; 3) have its profile on the upper face of the lesion within the inclusion zone. The estimated total number of axons was calculated by multiplying the number of axons counted by the inverse of the proportion of the area sampled (Gundersen, 1986; Peterson, 1999; West, 1993). In the ipsilateral ventromedial tract, all BDA-labeled axons of passage were counted. Axons were quantified in a total of 5 sections (0.5 mm apart) within the C5 and L4 levels for the T10 thoracic lesions and the C3 and C8 levels for the C7 cervical lesions.

2.1.6. IBA-1 immunohistochemistiy—For detection of activated microglia within the monkey cortex, IBA-1 immunohistochemistry was performed. Forty-micron transverse sections through the monkey motor cortex were blocked with normal goat serum in TBS + 0.25% triton-x. Sections were then incubated overnight at 4C in blocking solution containing rabbit anti-IBA-1 (Wako; 1 μg/ml). Following washes in TBS, sections were incubated for 2 h at room temperature in blocking solution containing Alexa-594 conjugated goat anti-rabbit secondary antibodies (Life Technologies; 1:500). Sections were washed in TBS, mounted on gelatin-subbed slides and coverslipped with Flouromount G. Images from 4 sections per subject were obtained using an Olympus FV1000 laser scanning confocal microscope with a 60 × objective. Percent area occupied by IBA-1 immunolabeling was determined using Image J. Mean density per subject was calculated for each cortex.

2.2. Experimental design, rodent study

As presented in Results, analysis of primate data indicated a 4-fold increase in the number of BDA-labeled ventral CST axons both above and below a spinal cord lesion. This increase was not seen when the motor cortex injections were delayed 2 months after the lesion surgery. To gain insight into the mechanism of such changes in axonal labeling we performed a similar experiment in rats.

The following groups were examined: Group 1, Intact (N = 6); Group 2, Bilateral C5 dorsal CST lesion + immediate motor cortex tracer injection (Lesion/No Delay Trace group; N = 6); Group 3, Bilateral C5 dorsal CST lesion + 2 week delayed motor cortex injection

(Lesion/Delayed Trace; N = 6). In each case, the ventral CST was spared to enable compensatory sprouting to removal of the dorsal CST. Each rat received injections of two types of tracer: BDA and lentivirally-administered Green Fluorescent Protein (GFP). BDA is actively transported in the axon (Glover et al., 1986; Schmued et al., 1990), whereas the GFP transport coefficient is consistent with diffusion, as determined by FRAP experiments (Konzack et al., 2007). In addition, we performed a time course study to estimate the rate of BDA transport when administered at the time of lesion or delayed. BDA was injected into the rat motor cortex immediately or delayed by 2 weeks and the animals were sacrificed 3 days (3-day group; N = 6) or 5 days (5-day group; N = 6) later. Spinal cord sections were then analyzed at identical distances from the obex/C1 interface. All procedures adhered to IACUC guidelines and animals had free access to food and water throughout the study.

2.2.1. Detailed methods, rodent study

2.2.1.1. Spinal cord lesion.: Adult fisher 344 female rats (125–150 g) were anesthetized with a mixture of ketamine (25 mg/ml), xylazine (1.3g/ml) and acepromazine (0.25 mg/ml). A laminectomy was performed at the C4 vertebral body corresponding to spinal level C5. A tungsten wire knife (Kopf) was stereotaxically lowered into the spinal cord 1.0 mm and extruded 3.0 mm to specifically transect the dorsal CST bilaterally (Fig. 5). Following SCI, rats were given 0.5 mg/kg ampicillin and 1.1 mg/kg banamine. Rats displayed no obvious adverse affects post-lesion. This type of lesion transects the dorsal CST from both cortices, but spares the ventral CST from both cortices descending within the ventral funiculus (Fig. 5).

2.2.1.2. Production of lendviral vectors for “passive” CST tract tracing.: Lentiviral vectors were constructed as previously described (Blesch, 2004). The complete enhanced GFP (GFP) cDNA plus Kozak consensus sequence was cloned into the *Bam*H1 and *Eco*R1 sites of the vector pENTR (Invitrogen) that was recombined into a lentiviral vector driven by the cytomegalovirus/beta-actin hybrid promoter (Niwa et al., 1991). High titer stocks of lentivirus were prepared by ultracentrifugation and titers were determined by infection of HEK293T cells. In addition, vector stocks were assayed for p24 antigen levels using a HIV-1 p24-specific ELISA kit (DuPont), as previously described (Naldini et al., 1996). Lenti-GFP vector preparations contained 106 μg/ml p24 and 1 × 10^8 IU/ml.

2.2.1.3. CST tract tracing with BDA or GFP.: Immediately or 14 days following bilateral cervical dorsal column lesions, a craniotomy was performed to expose the right motor cortex. A 10% solution of 10,000 molecular weight lysine-fixable biotinylated dextran-amine (BDA) was prepared by re-suspending 5 mg BDA in 50 μl of 1×10^8 IU/ml GFP expressing lentivirus. To label CST axons by active (BDA) and passive (GFP) transport, the BDA/lentivirus-GFP mixture was injected into 18 sites spanning the hindlimb motor cortex, as described previously (Weidner et al., 2001). Injection coordinates were rostral/caudal: every 0.05 cm; Bregma +0.10 to −0.30 cm and medial/lateral: Bregma −0.25 cm and −0.35 cm. The volume per site was 300 nl. injected with a picospritzer at a rate of 1 μl/min. Animals (N = 6/group) were sacrificed 3, 5, or 24 days after tracing.

2.2.1.4. Tissue preparation, immunohistochemistry and axonal quantification.: Rats were deeply anesthetized and perfused transcardially with 250 ml of 4% PFA. Spinal cord and brain tissue was post-fixed overnight in 4% PFA at 4 °C and cryoprotected in 30% sucrose 2–3 days at 4 °C. Spinal cords were blocked in the coronal plane and sectioned on a freezing microtome set at 40 μm intervals. Serial sections were collected into cryoprotectant and stored at −20 °C. Spinal cord sections were immunolabeled for BDA, described above, or for GFP. For GFP labeling, sections were quenched in 0.6% H_2O_2 in TBS, then blocked in 5% normal goat serum in TBS + 0.25% triton. Sections were incubated in rabbit anti-GFP (0.1 μg/ml, Life Technologies) overnight at 4 °C, washed in TBS, incubated in goat anti-rabbit Poly HRP (1:10, Millipore) for 1 h at room temperature and developed with DAB + $NiCl_2$ as per BDA staining. BDA and GFP-labeled axons were quantified within the dorsal columns above the lesion at cervical C3 segment (4 sections per animal) using the same stereological methods stated in the primate methods section. For quantification of the ventral CST, every BDA and GFP-labeled axon was counted above the lesion at C3 and below the lesion at cervical C6 spinal segment (4 sections per level per animal).

2.2.1.5. BDA uptake quantification.: To estimate the number of BDA-labeled neuronal cell bodies within the cortex, a 200 μm × 200 μm box was placed within layer V in the path of the injection tract or immediately adjacent to the injection tract. Every BDA-labeled cell body was counted in a series of 6 sections spanning the cortical injection coordinates.

2.2.1.6. Time course of axonal growth.: To access the rate of BDA transport, animals (N = 6/group for each of Intact group, Delay Group, and No Delay group) were sacrificed at 3 or 5 days post-cortical injections. 40 μm serial transverse sections were obtained from the obex/C 1 spinal border to 5 mm caudal and labeled for BDA. Every 0.5 mm (3-day survival) or 1.0 mm (5-day survival) the total number BDA-labeled axons were counted within the ventral CST tract. Mean numbers of ventral CST axons within each group at each level were plotted using Prism 5 software. For qualitative visualization of BDA-labeled axons (Fig. 10 A–C), a separate set of animals was used (N = 3/group). 30 μm serial sagittal sections were labeled for BDA. The entire extent of each axon was traced using Neurolucida software for each adjacent section. Traces from adjacent sections were then superimposed using Adobe Illustrator software.

2.2.1.7. Image capture and processing.: Light level images were captured using an Optronic Microfire A/R digital camera. Fluorescent images were captured with an Olympus Fluoview FV1000 confocal microscopy. All images were imported into Photoshop CS2 (Adobe) and brightness and contrasted optimized for image clarity.

2.2.1.8. IBA-1 immunohistochemistry.: For detection of activated microglia within the rat cortex, IBA-1 immunohistochemistry was performed. Forty-micron transverse sections through the monkey motor cortex were blocked with normal goat serum in TBS + 0.25% triton-x. Sections were then incubated overnight at 4 °C in blocking solution containing rabbit anti-IBA-1 (Wako; 0.2 μg/ml). Following washes in TBS, sections were incubated for 1 h at room temperature in blocking solution containing biotin conjugated goat anti-rabbit secondary antibodies (Vector Labs, 1:200). Sections were washed in TBS and incubated for

1 h at room temperature in ABC elite reagent (Vector Labs, 1:100). Sections were washed in TBS and developed with DAB + $NiCl_2$ as per BDA staining. Images from 4 sections per subject were obtained using a Keyence-all-in one imaging system with a 20 × objective. Percent area occupied by IBA-1 immunolabeling was determined using Image J.

2.2.1.9. Statistical analyses.: Multiple-group comparisons were assessed by ANOVA with a significance criterion of 95% using Prism 5 software. Post hoc differences were testing by Fisher's least-square difference. Observers were blinded to group identity in all assessments.

3. Results

3.1. Primate studies

All subjects survived the experimental procedure and were returned to their home enclosures approximately one week after the procedure. Lesions resulted in deficits of fine, but not gross, features of locomotion and persistent deficits in right hand (C7 lesions) or right foot (T10 lesions). Functional outcomes following these lesion models have been published previously and are not further addressed here (Courtine et al., 2005; Nout et al., 2012a; Nout et al., 2012b; Rosenzweig et al., 2010).

3.1.1. Increased numbers of right ventral CST axons after right dorsolateral CST lesions—BDA was injected into the right motor cortex to anterogradely label CST axons immediately after right T10 dorsolateral CST lesions (Fig. 1A). Lesions removed the vast majority of spinal cord parenchyma in the region subjected to the wire knife lesion (Fig. 1B). Lesion extent for these subjects has been described previously (Courtine et al., 2005). Notably, 3 months following right CST lesions, we observed a significant, 4.5-fold increase in the number of BDA-labeled CST axons in the right ventral CST at the L4 level compared to the number of ventral CST axons at L4 in intact monkeys ($p = 0.02$; Fig. 2B): Intact 27.9 ± 1.9 axons ± SEM; Lesion/No Delay Trace group 128 ± 36 axons. Axonal quantification 14 spinal segments above the lesion at C4 displayed a similar increase ($p = 0.02$; Fig. 2B): Intact 7.8 ± 2.8 axons; Lesion/Delayed Trace group 18 ± 3 axons. There were fewer labeled axons at cervical levels than at lumbar levels due to transport of BDA past the cervical spinal cord at this 3-month post-tracer injection time point.

These results suggest either: 1) that there is an extensive, 4-fold increase in the growth of new ventral CST axons located in white matter along an extended rostral-to-caudal length of the spinal cord following removal of 90% of CST axons in the dorsolateral fasciculus, or 2) that ventral CST axons are more readily detected after injury than in intact animals, possibly due to enhanced BDA transport brought about by injury.

To determine whether the delay between CST injury and BDA tracer injection can impact the transport and detection of BDA-labeled axons in the spinal cord, we performed additional right dorsal quadrant CST lesions in monkeys at C7, but delayed cortical BDA tracer injections by 2 months. Now, 3.5 months following right CST lesions, we no longer detected a significant increase in the number of BDA-labeled CST axons in the right ventral CST at either C4 ($p = 0.9$) or C8 ($p = 0.6$) in lesioned monkeys compared to intact monkeys (Fig. 3): C8 Intact, 178 ± 15 axons; Lesion/Delayed Trace group, 165 ± 15 axons ($p = 0.9$);

C3 Intact, 212 ± 10 axons; Lesion/Delayed Trace group, 209 ± 11 axons ($p = 0.6$). These results suggest that the timing of tracer injection may be critical to interpreting axonal labeling following injury.

3.1.2. Transient, bilateral activation of monkey motor cortex microglia—

Since in these experiments the right motor cortex is less proportionately affected by the right-sided spinal cord lesion (~10% of the total descending CST; Fig. 1A), we aimed to determine whether an injury signal is presented to the right motor cortex. Ionized calcium binding adapter protein 1 (IBA-1), a marker for microglia, has been shown to increase within the brain following spinal cord injury (Schwab et al., 2001). We assessed microglial activation in the Lesion/No Delay Trace (to CST tracing) group of monkeys that underwent right C7 hemisection lesions and were sacrificed 6–12 days later (N = 4; (Rosenzweig et al., 2010), and in Lesion/Delay Trace monkeys (traced 2 months post-lesion) that were sacrificed two months post-lesion (N = 4). The amount of IBA-1 immunolabeling was significantly greater in the short-term (6–12 day post-lesion) monkeys in both the left and right motor cortices compared to non-lesioned or 2-month lesioned monkeys ($p < 0.05$; Fig. 4). These results suggest that following a right-sided spinal cord lesion, both left and right motor cortices receive a transient injury signal. The results of IBA-1 labeling are presented to demonstrate that both motor cortices are affected by a unilateral CST lesion in the monkey; whether microglial activation or some other mechanism is *causally* related to enhanced axonal transport will be a subject of future studies.

3.2. Rodent studies

3.2.1. Increased BDA labeling in spared ventral CST axons following SCI in the rat—

To gain insight into mechanisms underlying transient increases in ventral CST BDA labeling in C7-lesioned rhesus monkeys, we performed parallel experiments in rats. In the monkey, both motor cortices contribute axons to the lesioned right dorsolateral corticospinal projection: 90% of axons in the right dorsolateral CST arise from the left motor cortex, and 8% from the right motor cortex (Lacroix et al., 2004; Rosenzweig et al., 2009). In rats, fewer than 1% of axons in the right dorsal CST arise from the right motor cortex; therefore, to deliver an injury signal to both cortices, we performed bilateral dorsal column lesions at C5 in rats, sparing the ventral CST (Fig. 5). BDA tracers were then injected either immediately following the lesion (Lesion/No Delay Trace group) or 2 weeks after lesions were placed (Lesion/Delayed Trace group), as in monkey experiments. Findings were compared to BDA injections in Intact animals. Furthermore, we traced the CST by co-injection of two independent tracers: BDA, an actively transported tracer, and lentivirus GFP, a tracer that passively diffuses through the cell (Konzack et al., 2007), exclusively labeling axons in the spinal cord (Fig. 6). When quantified two weeks later, the number of BDA-labeled axons within the ventral CST was significantly increased ($p < 0.05$, ANOVA) at C5 in the Lesion/No Delay Trace group: Intact, 109 ± 26 axons (± SEM); Lesion/No Delay Trace, 314 ± 108 axons, Lesion/Delayed Trace group, 112 ± 33 axons (Fig. 7)

3.2.2. No difference in GFP labeling of spared ventral CST axons following SCI in the rat—

Since BDA is actively transported within the axon (Glover et al., 1986; Terasaki et al., 1995), we also labeled CST axons with the diffusible label, GFP, that does

not require axonal transport (Konzack et al., 2007). Co-injection of a mixture of GFP-expressing lentivirus and BDA did not impair the visualization of either tracer. Most axons were co-labeled with GFP and BDA within the dorsal CST and the spinal gray matter. Quantification of the number of GFP-labeled ventral or dorsal CST axons indicated there were no significant differences when the GFP-expressing lentivirus was injected in Intact rats (Dorsal: 3870 ± 1420; Ventral: 37 ± 14), Lesion/No Delay Trace group (Dorsal: 3330 ± 560; Ventral: 33 ± 4) or Lesion/Delayed Trace group (tracer injection delayed 2 weeks after dorsal CST transection; Dorsal: 4010 ± 1400; Ventral: 35 ± 10) (Fig. 8). These findings suggest that following dorsal column CST lesions, spared ventral CST axons do not exhibit long distance growth, but instead increase transport of the BDA tracer.

3.2.3. Transient, bilateral activation of rat motor cortex microglia after unilateral SCI—In monkey studies above, we found bilateral cortical activation elicited by unilateral SCI, as reflected by IBA-1 labeling; we interpret these findings to indicate that both cortices exhibit an injury signal that may generate enhanced axonal transport. Future studies will determine whether microgial activation or some other mechanism accelerates axonal transport. To determine whether bilateral cortical activation also occurs in the rat model, we performed C5 unilateral lesions as above. Rats underwent dorsal column lesions and were sacrificed 3 and 14 days post-lesion (N = 3/group). The amount of IBA-1 immunolabeling was significantly greater in the short-term (3 day post-lesion) rats in motor cortex compared to non-lesioned or 14-day lesioned rats ($p < 0.05$; Fig. 9). These results suggest that following a right-sided spinal cord lesion, both left and right motor cortices receive a transient injury signal (Schwab et al., 2001).

3.2.4. Cortical neuronal uptake of BDA is constant—To determine whether changes in BDA uptake in layer 5 cortical neurons might account for the observed differences in the number of BDA-labeled ventral CST axons in the spinal cord, we quantified BDA-labeled neurons in the motor cortex in Intact, Lesion/No Delay Trace and Lesion/Delayed Trace groups (Fig. 10). No significant differences were detected in the total number of BDA-labeled layer V neurons ($p = 0.5$).

3.2.5. SCI results in a transient increase in axonal transport of BDA within spared rat ventral CST axons—The preceding results demonstrate that a greater number of ventral CST axons are labeled with BDA when tracer is injected at the same time as dorsal column transection compared to tracer injection after a several week (rat) or month (primate) delay. This finding suggests either that spared ventral CST axons upregulate transport of BDA following lesion of the main dorsal CST component, or that there is an actual transient increase in number of ventral CST axons that are subsequently retracted. The latter possibility is excluded by the fact that the total number of axons does not change as a function of time when detected by the passive tracer GFP. To confirm that axonal transport increases, we injected BDA either immediately or 2 weeks following placement of dorsal column lesions and examined whether BDA moved down the axon more rapidly in the Lesion/No Delay group: the total number of BDA labeled axons was quantified either 3 or 5 days post-tracer injection from the obex caudally (Fig. 11). Three days post-tracer injection, the number of axons labeled at the obex was equal among all groups, but became

progressively higher at caudal distances in the Lesion/No Delay group, indicating that BDA moved down axons more rapidly in the Lesion/No Delay group compared to Intact and Lesion/Delayed group animals (Fig. 11 A; $p < 0.05$ ANOVA at distances of 1.5 and 2 mm; post-hoc Fischer's showed significant differences between Lesion/No Delay group compared to Intact and Lesion/Delayed groups). By 5 days post-tracer injections, the total number of axons labeled in each group at these distances had increased, but remained significantly higher in the Lesion/No Delay group at all distances measured (Fig. 11B; ANOVA $p < 0.01$) at distances of 0–4 mm from the obex). Thus, BDA more rapidly fills axons when injected at the time of injury than in the intact state or when injected two weeks after an injury. BDA movement down the axon is equivalent in the Intact and Lesion/Delayed Trace groups (Fig. 11), indicating that BDA transport returns to normal by two weeks post-tracer injection.

4. Discussion

Findings of this study demonstrate that ventral corticospinal axons exhibit transient increases in transport of BDA following injury, paralleling increases in axonal transport observed in successfully regenerating peripheral axons (Hausott and Klimaschewski, 2016; Hoffman, 2010). Despite these injury-related increases in axonal transport, CNS axons do not successfully regenerate, due to mechanisms that have been identified: inhibitors associated with myelin (Rao and Pearse, 2016; Schwab and Strittmatter, 2014), deposition of an inhibitory extracellular matrix at the lesion site (Busch and Silver, 2007; Dell'Anno and Strittmatter, 2017; Fawcett, 2015), and incomplete upregulation of intrinsic neuronal growth programs (Blackmore, 2012; He and Jin, 2016; Moore and Goldberg, 2011). Failure to upregulate axonal transport may in fact not be a limiting factor in CNS regeneration, given findings of the present study.

A notable feature of the present set of findings is that one might initially have mistakenly attributed the increased labeling of ventral CST axons in primates after dorsolateral CST lesions to new axonal growth. Our skepticism was generated by the observation that increased numbers of axons were also observed in *cervical* segments remote from the injury, in *white matter* that would be predicted to limit long-distance axonal growth (Schwab and Strittmatter, 2014). Further investigation, returning to rodent models, supported the alternative explanation that BDA transport was increased in ventral CST axons. Yet ventral CST axons have been reliably demonstrated to sprout after lesions of the majority dorsal CST (Weidner et al., 2001), but this sprouting occurs in host *gray matter* that is free of high levels of myelin-associated inhibitors. Indeed, terminal collateral sprouting of corticospinal axons in gray matter is associated with functional improvement in rodent models (Carmel et al., 2010; Lee et al., 2010; Weidner et al., 2001). Our findings caution that the timing of tracer injection may be critical in interpreting axonal sprouting or regeneration.

How might a cortical neuron that projects through the non-lesioned, ventral corticospinal tract increase axonal transport when injury occurs to the majority dorsal or dorsolateral projection? First, ventral corticospinal axons may be collateral branches of dorsal CST lesioned axons. Second, spinal cord lesions activate microglia and astrocytes both in the cortex that gives rise to the transected axons, and in the contralateral hemisphere containing

the cell bodies of the non-lesioned ventral corticospinal neuron in our primate model (Lacroix et al., 2004; Rosenzweig et al., 2009) (Fig. 4). Reactive astrocytes and activated microglia can increase glutamate release, generate local ionic changes and increase free radical release that may in turn activate the soma of the ventral corticospinal neuron (Kost-Mikucki and Oblinger, 1991; Park et al., 2004; Schwab et al., 2001). These inflammatory changes may be causally related to generating a state of enhanced axonal transport in the neuronal soma; however, future experiments focused specifically on inflammatory mechanisms will be required to draw clear mechanistic conclusions.

A limitation of the primate component of this study was the use of two different lesion levels to study acute and delayed tracer injections, respectively, and the small number of subjects studied at the cervical level. As stated on page 6, it would have been optimal to study a complete set of animals with lesions at a single spinal level, but in the course of pursuing other, therapeutically-driven studies in the primate model, we made a programmatic decision to change the lesion model from T10 to C7. Recognizing the importance of determining whether changes in axonal transport might account for increased numbers of spared ventral axons after acute tracer injections in primates, we performed additional, mechanistic studies in rodent models. It is possible that a factor other than axonal transport may have accounted for altered axonal numbers in primates at the lumbar vs. cervical levels, given the differing distances of these lesions from the neuronal soma (Grafstein, 1975), or hypothetically differing branching patterns of axons at cervical vs. lumbar levels. However, these possibilities seem unlikely, given the precise replication of altered axonal numbers in rodent studies that were associated with differences in axonal transport.

5. Conclusions

Axonal transport is acutely increased in injured CNS axons, paralleling observations in regenerating PNS axons. Accordingly, a general ability to increase axonal transport may not be a factor limiting CNS regeneration. Other therapeutic targets such as the intrinsic growth state of the neuron, the injured environment and inflammatory responses may be more fruitful targets for intervention. Caution should be taken in interpreting changes in axonal numbers in studies of spinal cord injury: some findings of increased axonal numbers may be related to alterations in axonal transport of axonal tracers, rather than true new axonal growth.

Acknowledgments

This work was supported by the Veterans Administration (RX001045 and Gordon Mansfield Spinal Cord Injury Consortium), the NIH (R-01 NS042291 and R-01 NS104442), the Craig H. Neilsen Foundation, the Gerbic Family Foundation, the Dr. Miriam and Sheldon G. Adelson Medical Research Foundation, and the Bernard and Anne Spitzer Charitable Trust.

References

Bareyre FM, Kerschensteiner M, Raineteau O, Mettenleiter TC, Weinmann O, Schwab ME, 2004, The injured spinal cord spontaneously forms a new intraspinal circuit in adult rats. Nat. Neurosci 7, 269–277. [PubMed: 14966523]

Black MM, Lasek RJ, 1980 Slow components of axonal transport: two cytoskeletal networks. J. Cell Biol 86, 616–623. [PubMed: 6156946]

Blackmore MG, 2012 Molecular control of axon growth: insights from comparative gene profiling and high-throughput screening. Int. Rev. Neurobiol 105, 39–70. [PubMed: 23206595]

Blesch A, 2004 Lentiviral and MLV based retroviral vectors for ex vivo and in vivo gene transfer. Methods 33, 164–172. [PubMed: 15121171]

Busch SA, Silver J, 2007 The role of extracellular matrix in CNS regeneration. Curr. Opin. Neurobiol 17, 120–127. [PubMed: 17223033]

Carmel JB, Berrol LJ, Brus-Ramer M, Martin JH, 2010 Chronic electrical stimulation of the intact corticospinal system after unilateral injury restores skilled loco-motor control and promotes spinal axon outgrowth. J. Neurosci 30, 10918–10926. [PubMed: 20702720]

Courtine G, Roy RR, Raven J, Hodgson J, McKay H, Yang H, Zhong H, Tuszynski MH, Edgerton VR, 2005 Performance of locomotion and foot grasping following a unilateral thoracic corticospinal tract lesion in monkeys (Macaco, mulatto). Brain 128, 2338–2358 a journal of neurology. [PubMed: 16049043]

Dell'Anno MT, Strittmatter SM, 2017 Rewiring the spinal cord: direct and indirect strategies. Neurosci. Lett 652, 25–34. [PubMed: 28007647]

Fawcett JW, 2015 The extracellular matrix in plasticity and regeneration after CNS injury and neurodegenerative disease. Prog. Brain Res 218, 213–226. [PubMed: 25890139]

Forbes LH, Andrews MR, 2017 Restoring axonal localization and transport of transmembrane receptors to promote repair within the injured CNS: a critical step in CNS regeneration. Neural Regen. Res 12, 27–30. [PubMed: 28250734]

Galbraith JA, Gallant PE, 2000 Axonal transport of tubulin and actin. J. Neurocytol 29, 889–911. [PubMed: 11466477]

Glover JC, Petursdottir G, Jansen JK, 1986 Fluorescent dextran-amines used as axonal tracers in the nervous system of the chicken embryo. J. Neurosci. Methods 18, 243–254. [PubMed: 2432362]

Grafstein B, 1969 Axonal transport: communication between soma and synapse. Adv. Biochem. Psychopharmacol 1, 11–25. [PubMed: 4947251]

Grafstein B, 1975 The nerve cell body response to axotomy. Exp. Neurol 48, 32–51. [PubMed: 1102323]

Grafstein B, Murray M, 1969 Transport of protein in goldfish optic nerve during regeneration. Exp. Neurol 25, 494–508. [PubMed: 5362566]

Gundersen HJ, 1986 Stereology of arbitrary particles. A review of unbiased number and size estimators and the presentation of some new ones, in memory of William R. Thompson. J. Microsc 143, 3–45. [PubMed: 3761363]

Hausott B, Klimaschewski L, 2016 Membrane turnover and receptor trafficking in regenerating axons. Eur. J. Neurosci 43, 309–317. [PubMed: 26222895]

He Z, Jin Y, 2016 Intrinsic control of axon regeneration. Neuron 90, 437–451. [PubMed: 27151637]

Hoffman PN, 2010 A conditioning lesion induces changes in gene expression and axonal transport that enhance regeneration by increasing the intrinsic growth state of axons. Exp. Neurol 223, 11–18. [PubMed: 19766119]

Konzack S, Thies E, Marx A, Mandelkow EM, Mandelkow E, 2007 Swimming against the tide: mobility of the microtubule-associated protein tau in neurons. J. Neurosci 27, 9916–9927. [PubMed: 17855606]

Kost-Mikucki SA, Oblinger MM, 1991 Changes in glial fibrillary acidic protein mRNA expression after corticospinal axotomy in the adult hamster. J. Neurosci. Res 28, 182–191. [PubMed: 2033647]

Lacroix S, Havton LA, McKay H, Yang H, Brant A, Roberts J, Tuszynski MH, 2004 Bilateral corticospinal projections arise from each motor cortex in the macaque monkey: a quantitative study. J. Comp. Neurol 473, 147–161. [PubMed: 15101086]

Lee JK, Geoffroy CG, Chan AF, Tolentino KE, Crawford MJ, Leal MA, Kang B, Zheng B, 2010 Assessing spinal axon regeneration and sprouting in Nogo-, MAG-, and OMgp-deficient mice. Neuron 66, 663–670. [PubMed: 20547125]

Mar FM, Bonni A, Sousa MM, 2014a Cell intrinsic control of axon regeneration. EMBO Rep. 15, 254–263. [PubMed: 24531721]

Mar FM, Simoes AR, Leite S, Morgado MM, Santos TE, Rodrigo IS, Teixeira CA, Misgeld T, Sousa MM, 2014b CNS axons globally increase axonal transport after peripheral conditioning. J. Neurosci 34, 5965–5970. [PubMed: 24760855]

McEwen BS, Grafstein B, 1968 Fast and slow components in axonal transport of protein. J. Cell Biol 38, 494–508. [PubMed: 5664220]

Moore DL, Goldberg JL, 2011 Multiple transcription factor families regulate axon growth and regeneration. Dev. Neurobiol 71, 1186–1211. [PubMed: 21674813]

Naldini L, Blomer U, Gage FH, Trono D, Verma IM, 1996 Efficient transfer, integration, and sustained long-term expression of the transgene in adult rat brains injected with a lentiviral vector. Proc. Natl. Acad. Sci. U. S. A 93, 11382–11388. [PubMed: 8876144]

Niwa H, Yamamura K, Miyazaki J, 1991 Efficient selection for high-expression transfectants with a novel eukaryotic vector. Gene 108, 193–199. [PubMed: 1660837]

Nout YS, Ferguson AR, Strand SC, Moseanko R, Hawbecker S, Zdunowski S, Nielson JL, Roy RR, Zhong H, Rosenzweig ES, Brock JH, Courtine G, Edgerton VR, Tuszynski MH, Beattie MS, Bresnahan JC, 2012a Methods for functional assessment after C7 spinal cord hemisection in the rhesus monkey. Neurorehabil. Neural Repair 26, 556–569. [PubMed: 22331214]

Nout YS, Rosenzweig ES, Brock JH, Strand SC, Moseanko R, Hawbecker S, Zdunowski S, Nielson JL, Roy RR, Courtine G, Ferguson AR, Edgerton VR, Beattie MS, Bresnahan JC, Tuszynski MH, 2012b Animal models of neurologic disorders: a nonhuman primate model of spinal cord injury. Neurotherapeutics 9, 380–392 the journal of the American Society for Experimental NeuroTherapeutics. [PubMed: 22427157]

Park E, Velumian AA, Fehlings MG, 2004 The role of excitotoxicity in secondary mechanisms of spinal cord injury: a review with an emphasis on the implications for white matter degeneration. J. Neurotrauma 21, 754–774. [PubMed: 15253803]

Peterson DA, 1999 Quantitative histology using confocal microscopy: implementation of unbiased stereology procedures. Methods 18, 493–507. [PubMed: 10491280]

Rao SN, Pearse DD, 2016 Regulating axonal responses to injury: the intersection between signaling pathways involved in axon myelination and the inhibition of axon regeneration. Front. Mol. Neurosci 9, 33. [PubMed: 27375427]

Rosenzweig ES, Brock JH, Culbertson MD, Lu P, Moseanko R, Edgerton VR, Havton LA, Tuszynski MH, 2009 Extensive spinal decussation and bilateral termination of cervical corticospinal projections in rhesus monkeys. J. Comp. Neurol 513, 151–163. [PubMed: 19125408]

Rosenzweig ES, Courtine G, Jindrich DL, Brock JH, Ferguson AR, Strand SC, Nout YS, Roy RR, Miller DM, Beattie MS, Havton LA, Bresnahan JC, Edgerton VR, Tuszynski MH, 2010 Extensive spontaneous plasticity of corticospinal projections after primate spinal cord injury. Nat. Neurosci 13, 1505–1510. [PubMed: 21076427]

Scheff SW, Rabchevsky AG, Fugaccia I, Main JA, Lumpp JE Jr., 2003 Experimental modeling of spinal cord injury: characterization of a force-defined injury device. J. Neurotrauma 20, 179–193. [PubMed: 12675971]

Schmued L, Kyriakidis K, Heimer L, 1990 In vivo anterograde and retrograde axonal transport of the fluorescent rhodamine-dextran-amine, Fluoro-Ruby, within the CNS. Brain Res. 526, 127–134. [PubMed: 1706635]

Schwab ME, Strittmatter SM, 2014 Nogo limits neural plasticity and recovery from injury. Curr. Opin. Neurobiol 27, 53–60. [PubMed: 24632308]

Schwab JM, Frei E, Klusman I, Schnell L, Schwab ME, Schluesener HJ, 2001 AIF-1 expression defines a proliferating and alert microglial/macrophage phenotype following spinal cord injury in rats. J. Neuroimmunol 119, 214–222. [PubMed: 11585624]

Steward O, Zheng B, Tessier-Lavigne M, Hofstadter M, Sharp K, Yee KM, 2008 Regenerative growth of corticospinal tract axons via the ventral column after spinal cord injury in mice. J. Neurosci 28, 6836–6847. [PubMed: 18596159]

Terasaki M, Schmidek A, Galbraith JA, Gallant PE, Reese TS, 1995 Transport of cytoskeletal elements in the squid giant axon. Proc. Natl. Acad. Sci. U. S. A 92, 11500–11503. [PubMed: 8524791]

Weidner N, Ner A, Salimi N, Tuszynski MH, 2001 Spontaneous corticospinal axonal plasticity and functional recovery after adult central nervous system injury. Proc. Natl. Acad. Sci. U. S. A 98, 3513–3518. [PubMed: 11248109]

West MJ, 1993 New stereological methods for counting neurons. Neurobiol. Aging 14, 275–285. [PubMed: 8367009]

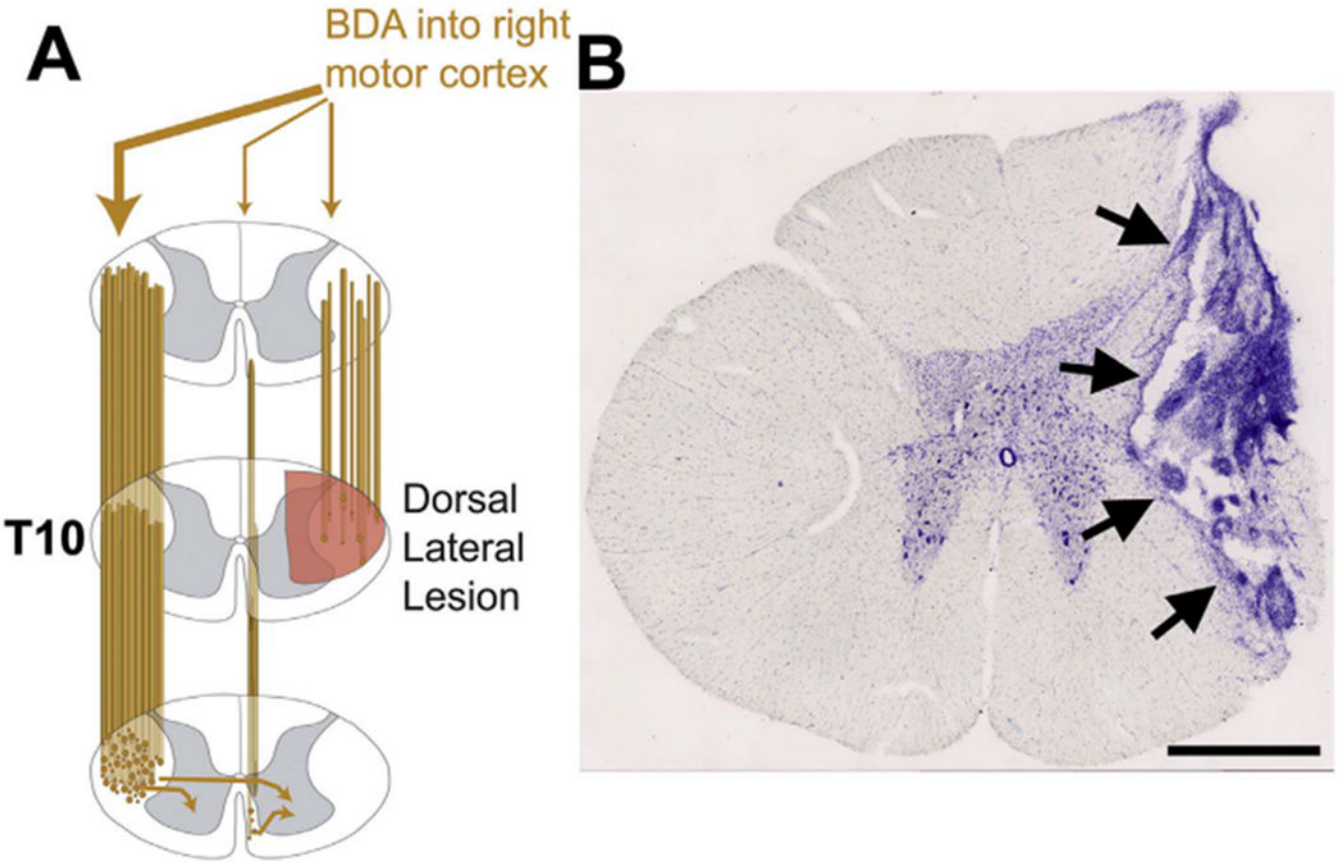

Fig. 1.

Right dorsolateral corticospinal tract lesion. (A) Schematic Illustrating spinal cord lesion at T10 and Injection of BDA tracer Into the motor cortex ipsilateral to the lesion, thereby labeling the ventral corticospinal tract in the Rhesus monkey. The lesion also transects approximately 10% of descending CST axons originating from the right motor cortex in the monkey. BDA was Injected Into the right motor cortex either at the same time that the lesion was placed, or 2 months later. (B) Nissl stain over transverse spinal cord section at T10 illustrating transection of the right dorsolateral quadrant. Scale bar: 2 mm.

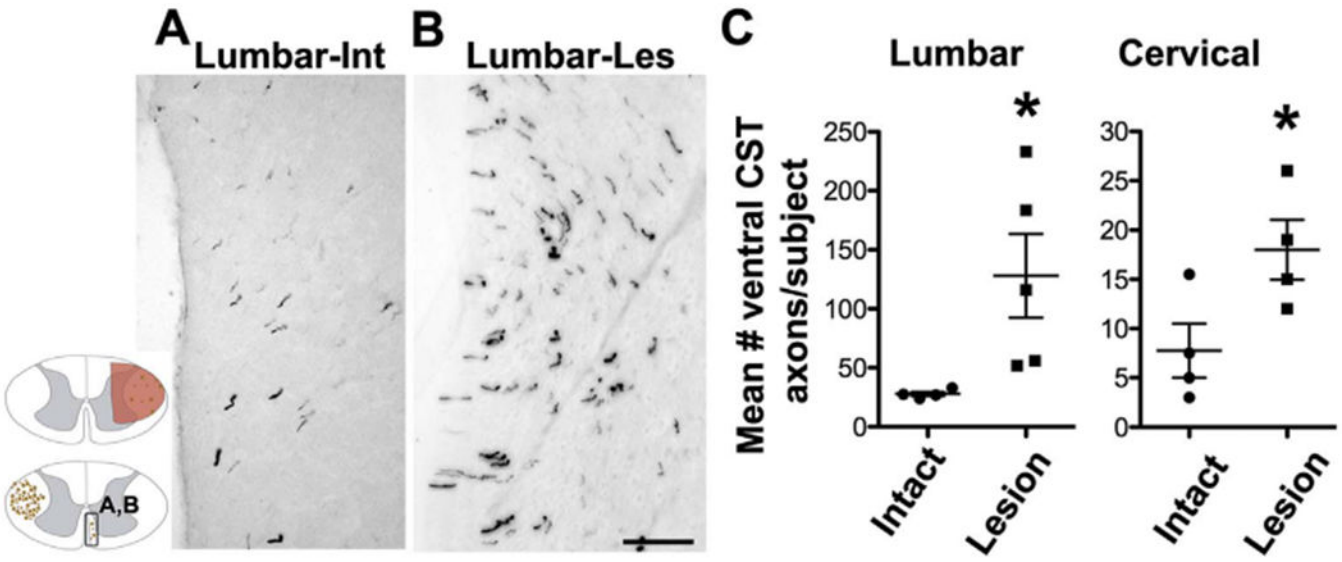

Fig. 2.

Increased numbers of BDA-labeled ventral CST axons after T10 dorsolateral quadrant lesions. (A) Photomicrograph of BDA-labeled ventral CST axons in an intact monkey at the L5 level. (B) T10 lesions results In an Increase In the number of ventral CST axons at the same level, when tracers are Injected at the same time that lesions are placed. (C) Quantification of the number of ventral CST axons at (C) C5 and (D) L5. Mean number of axons (N = 4–5/group) are plotted In C. *p < 0.05, Student's *t*-test. Scale bar A, B: 200 μm.

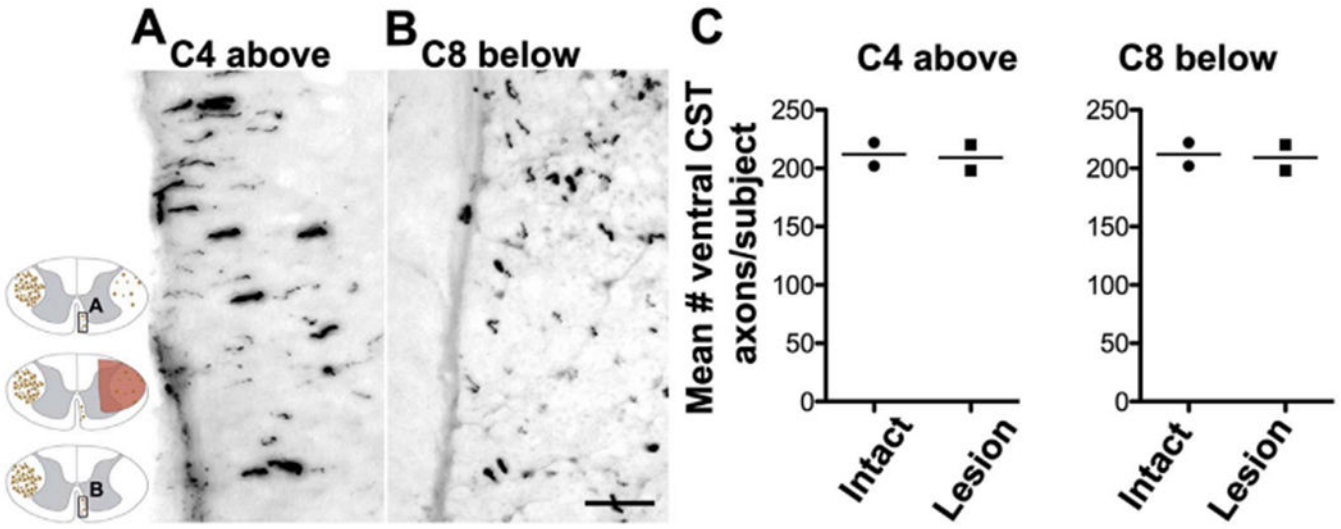

Fig. 3.

Numbers of BDA-labeled ventral CST axons are unchanged when tracer injections are delayed. (A) BDA labeled ventral CST axons in an intact monkey at C8. (B) Following C7 lesion and BDA tracer injections 6 weeks later, ventral CST axon numbers are unchanged when observed 2 months after tracer injections. (C). Mean number of axons (N = 2/group) are plotted in C. Scale bar 200 μm.

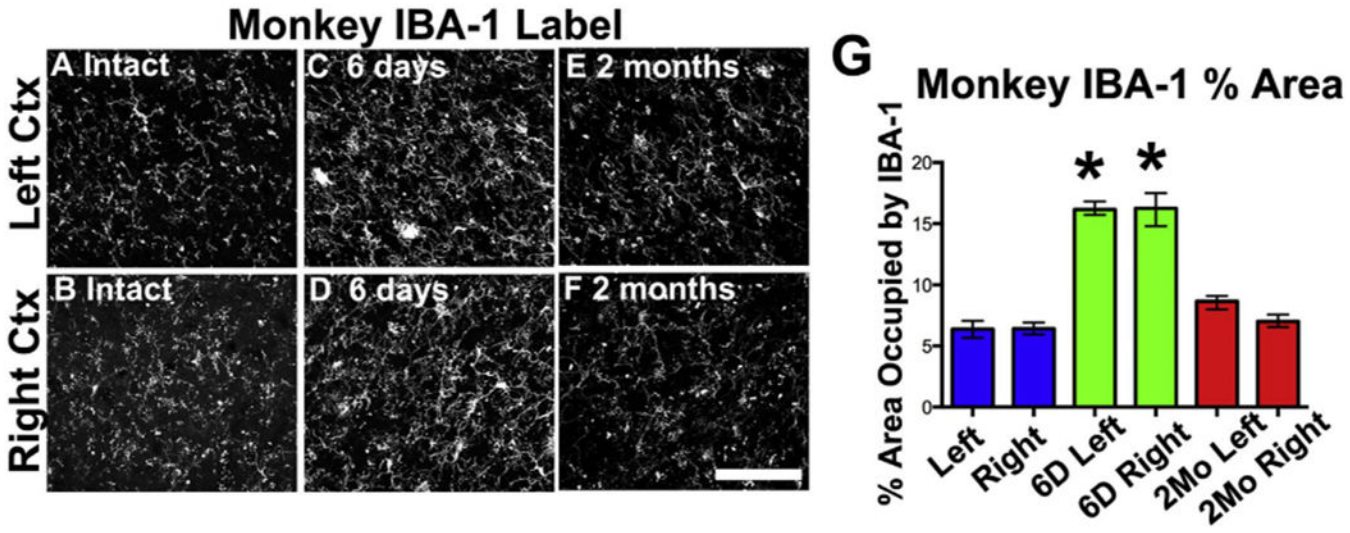

Fig. 4.

Transient microglial activation in bilateral cortices after SCI. Transverse sections of the rhesus monkey motor cortex immunolabeled for the microglial marker, IBA-1. (A, B) Confocal images of IBA-1 immunolabeling within layer V of intact cortex. (C, D) 6-days post-SCI, IBA-1 labeling in bilateral motor cortices is increased. (E, F) By 2 months post-SCI, IBA-1-labeling has returned to intact levels. (G) Mean density of IBA-1 ± standard error (N = 3/group) are plotted in D. Scale bar = 50 μm.

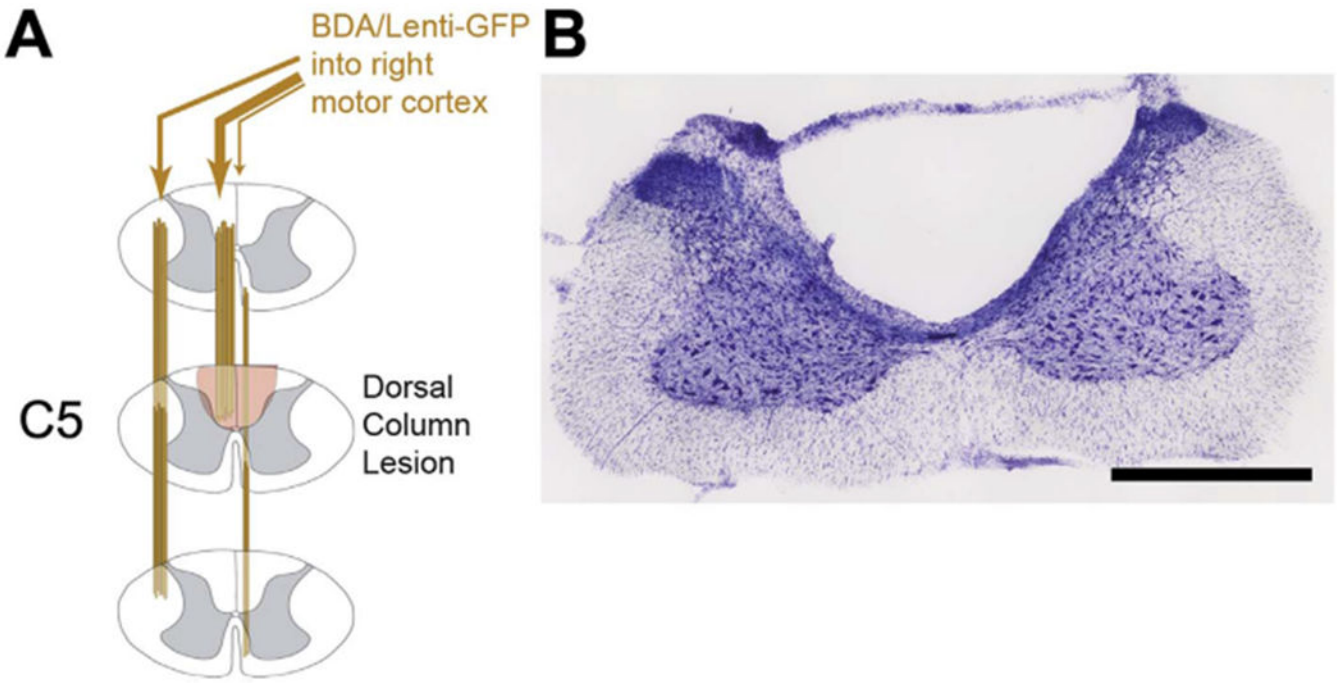

Fig. 5.

Rat bilateral dorsal column corticospinal tract lesions. (A) Schematic drawing of a bilateral dorsal column corticospinal spinal cord lesion. This lesion transects approximately 90% of descending CST axons from both cortices. Immediately or following a 2-week delay, a mixture of BDA and Lenti-GFP was injected into the right motor cortex. (B) Nissl stain of transverse spinal cord section at C5 illustrating bilateral dorsal column lesion. Scale bar: 2 mm. Scale bar: 1 mm.

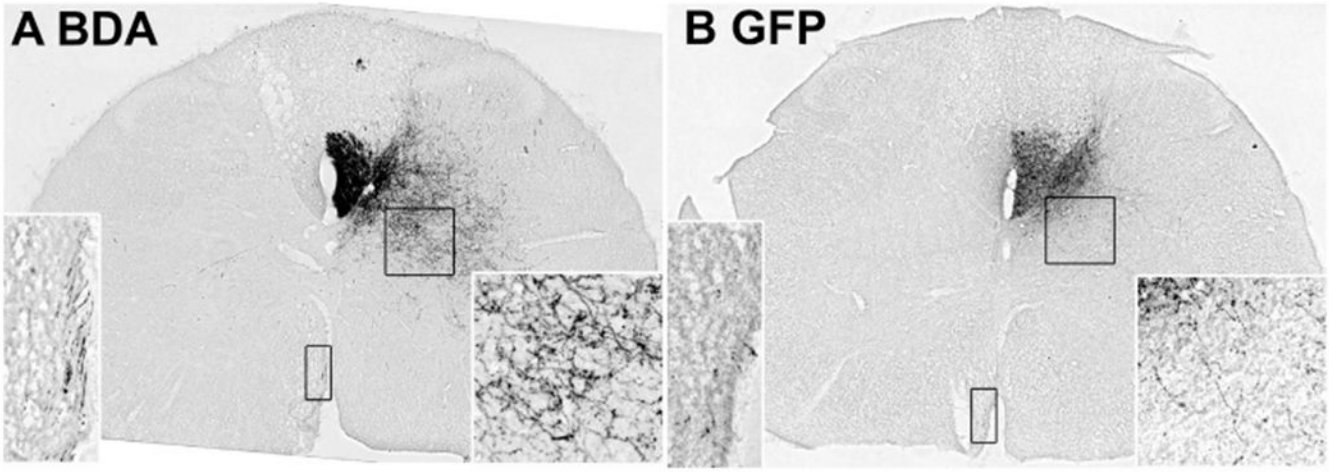

Fig. 6.

CST tracing with BDA and GFP. (A) Light level immunolabeling for BDA with insets showing labeling in ventro-medial CST and gray matter innervation. (B) Light level immunolabeling for GFP.

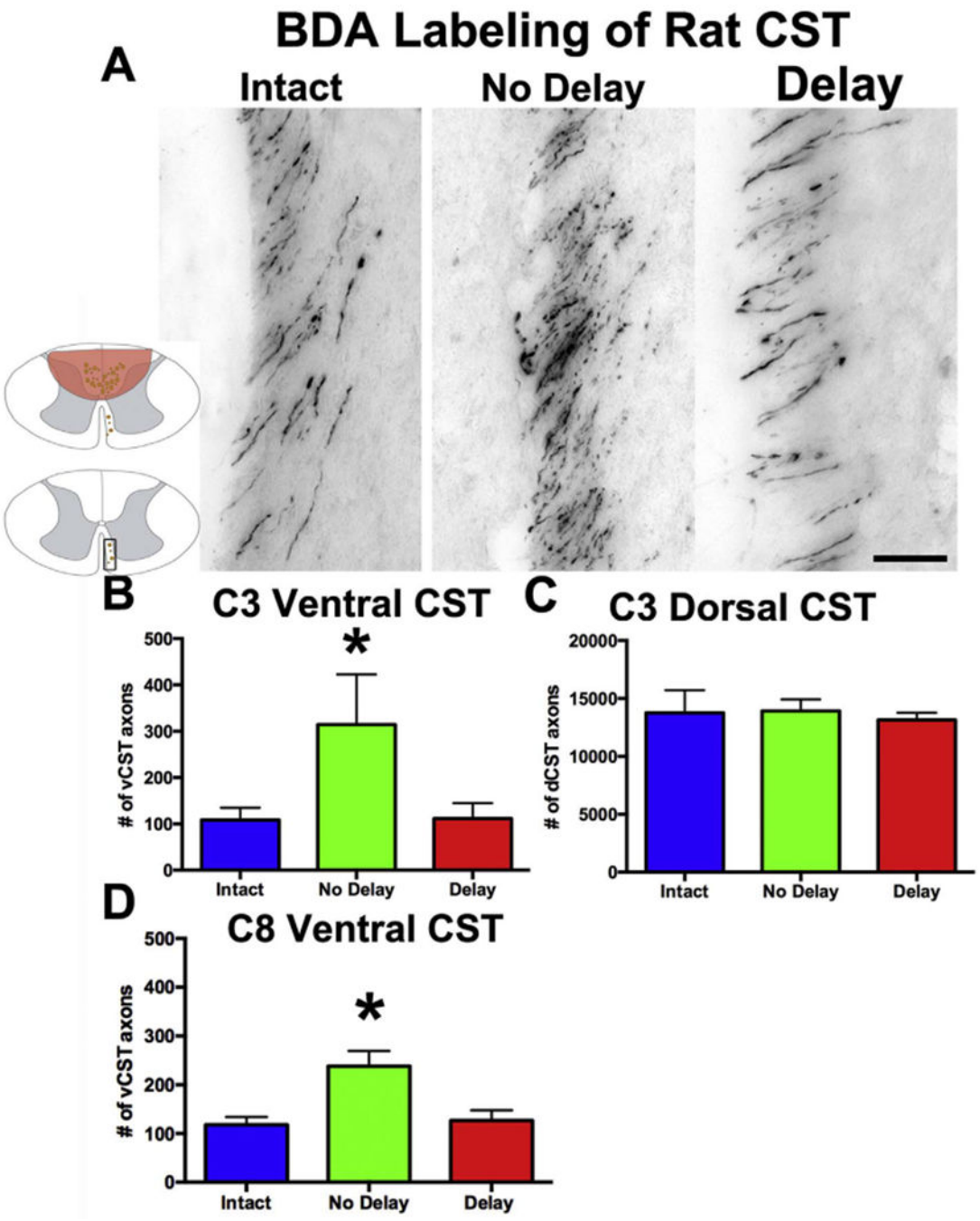

Fig. 7.

BDA-labeling of rat ventral CST axons depends on timing of tracer injections. (A) BDA-labeled right ventral CST axons in Intact group, Lesion/No Delay Trace group, and Lesion/Delay Trace group. (B–D) Quantification of BDA-labeled axons show significant increase in ventral CST at C3 and C8 spinal level among animals with No Delay between lesion and tracing, and a return to Intact values if tracer injections are delayed by two weeks (ANOVA, $p = 0.02$; No Delay group differs from both Intact and Delay Trace group, post-hoc Fischer's $p = 0.02$). However, number of BDA-labeled axons do not differ among groups in the dorsal

CST, quantified rostral to the lesion at C3, indicating similar tracer injections among groups ($p = 0.5$). Mean number of axons + standard error ($N = 6$/group) are plotted in B–D. Scale bar, 100 μm.

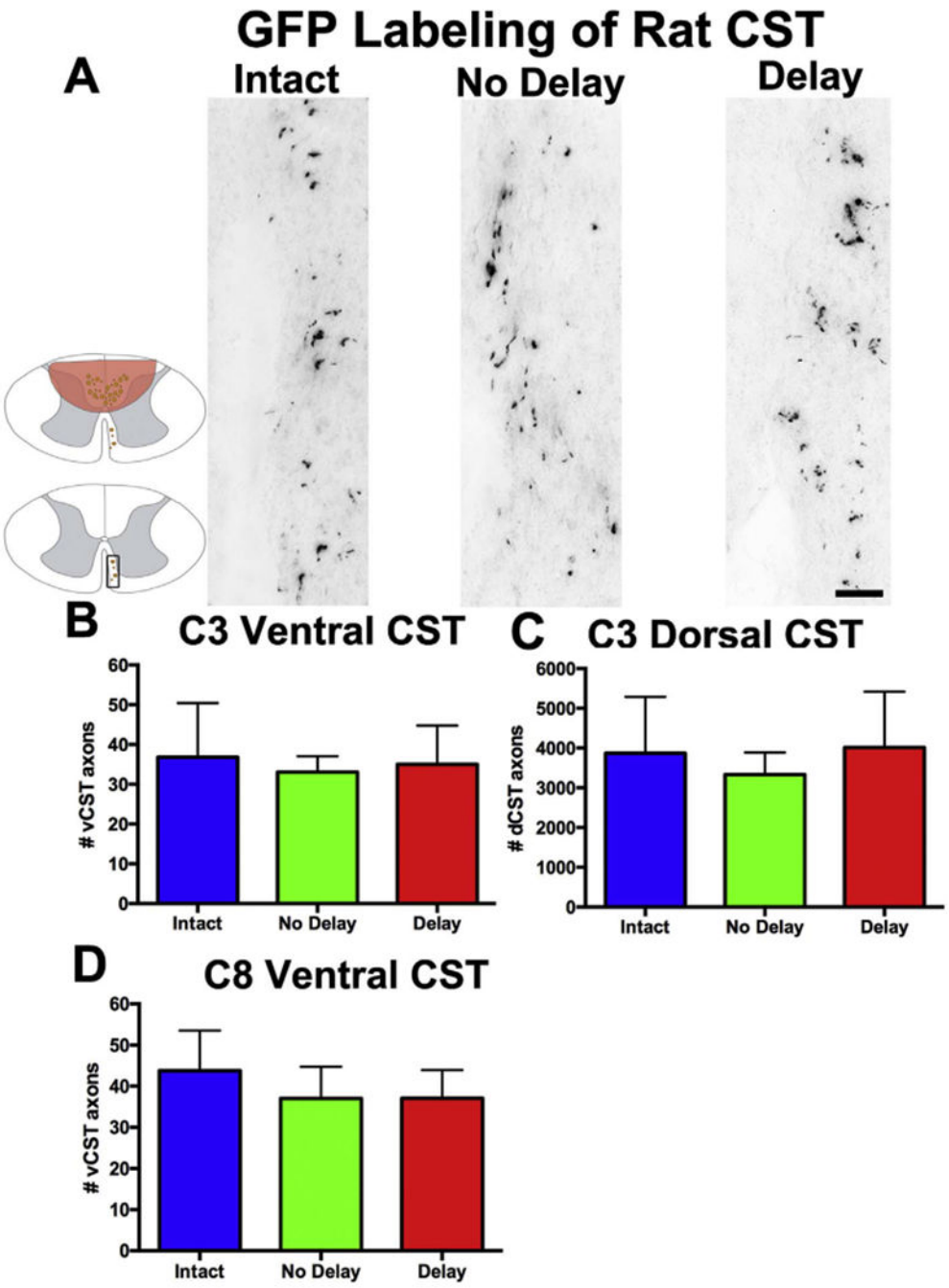

Fig. 8.

GFP labeling of rat ventral CST axons is consistent across times. (A) GFP immunolabeling of ventral CST traced in Intact group, Lesion/No Delay group, and Lesion/Delay group. (B–D) Quantification reveals no significant differences in the number of ventral or dorsal CST axons among groups quantified at C3 or C8 (ANOVA $p = 0.9$). Mean number of axons + standard error ($N = 6$/group) are plotted in B–D. Scale bar: 100 μm.

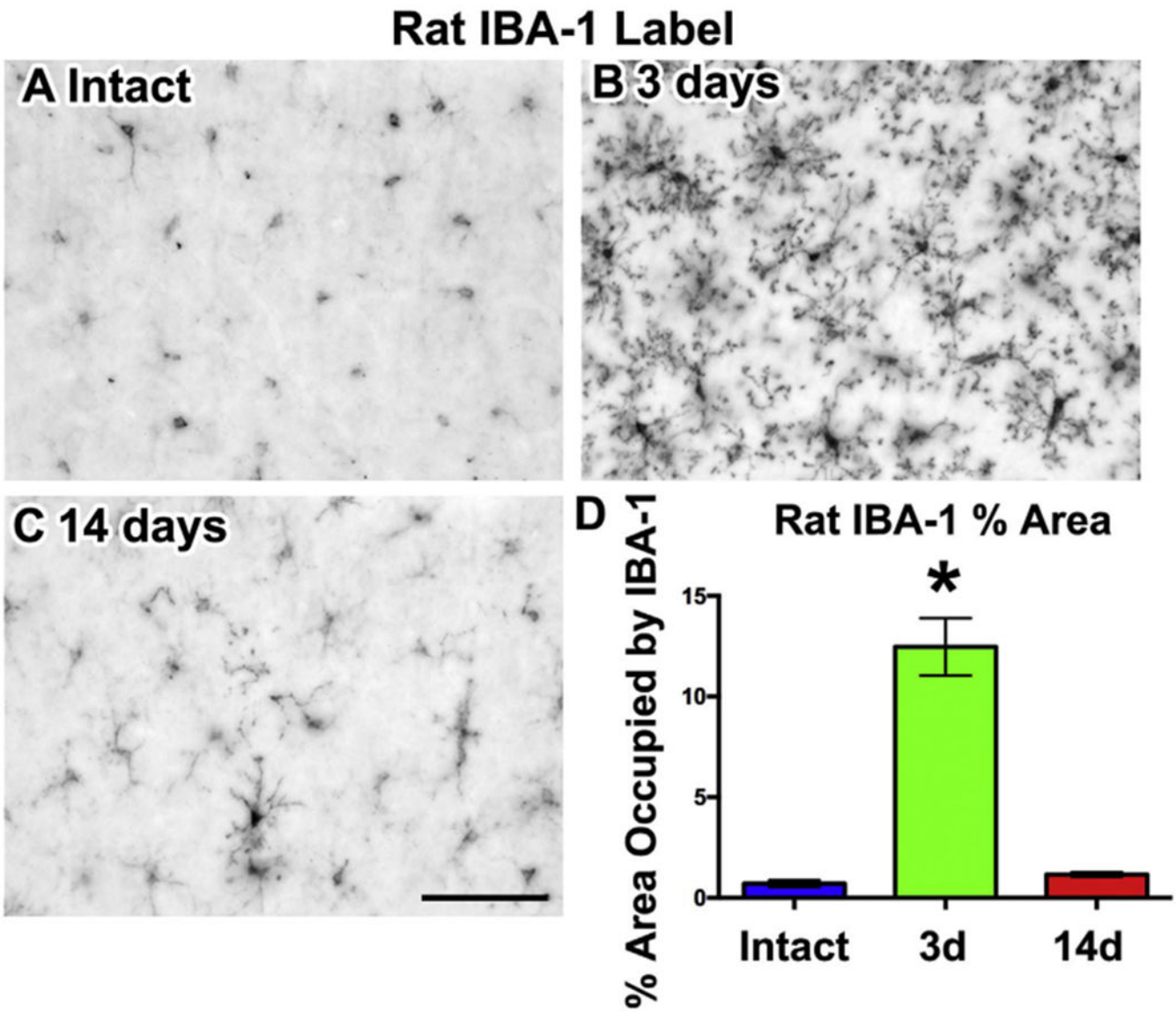

Fig. 9.

Transient microglial activation in motor cortex after SCI. Transverse sections of the rat motor cortex immunolabeled for the microglial marker, IBA-1. (A) Light level images of IBA-1 immunolabeling within layer V of intact cortex. (B) 3-Days post-SCI, IBA-1 labeling in motor cortex is increased. (C) By 14 days post-SCI, IBA-1-labeling has returned to intact levels. (D) Quantification of IBA-1 density. Mean density of IBA-1 ± standard error (N = 3/group) are plotted in D. Scale bar = 50 μm.

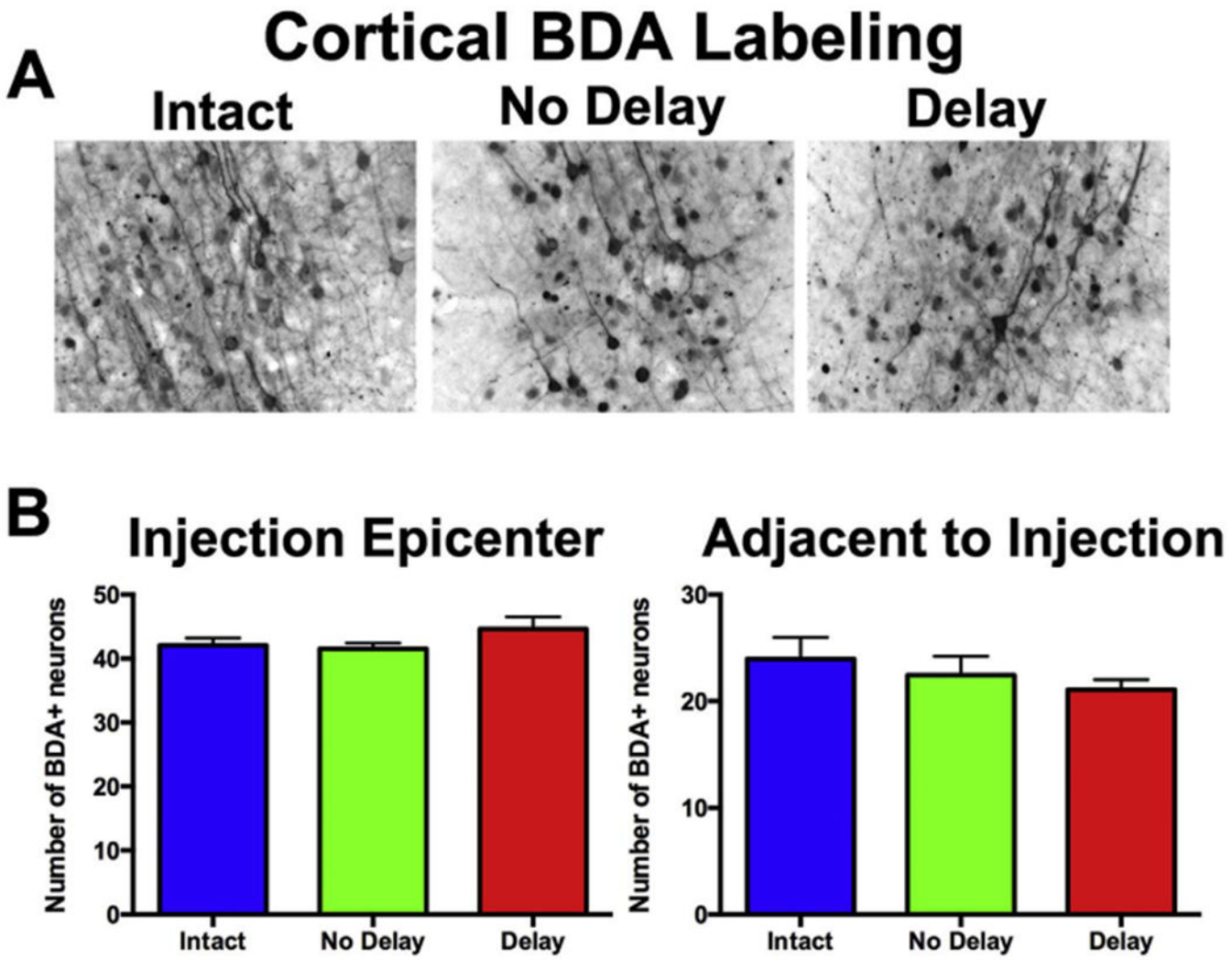

Fig. 10.

Cortical uptake of BDA is consistent. (A) BDA labeling of cortical neurons at injection sites of Intact group, Lesion/No Delay group, and Lesion/Delay group. (B) Quantification of the number of BDA-labeled neurons in the injection epicenter or in adjacent cortex (Mean + standard error). There are no significant group differences (ANOVA, Epicenter, $p = 0.3$; Adjacent, $p = 0.5$). Mean number of BDA labeled neurons + standard error (N = 4/group) are plotted in D. Scale bar, 100 μm.

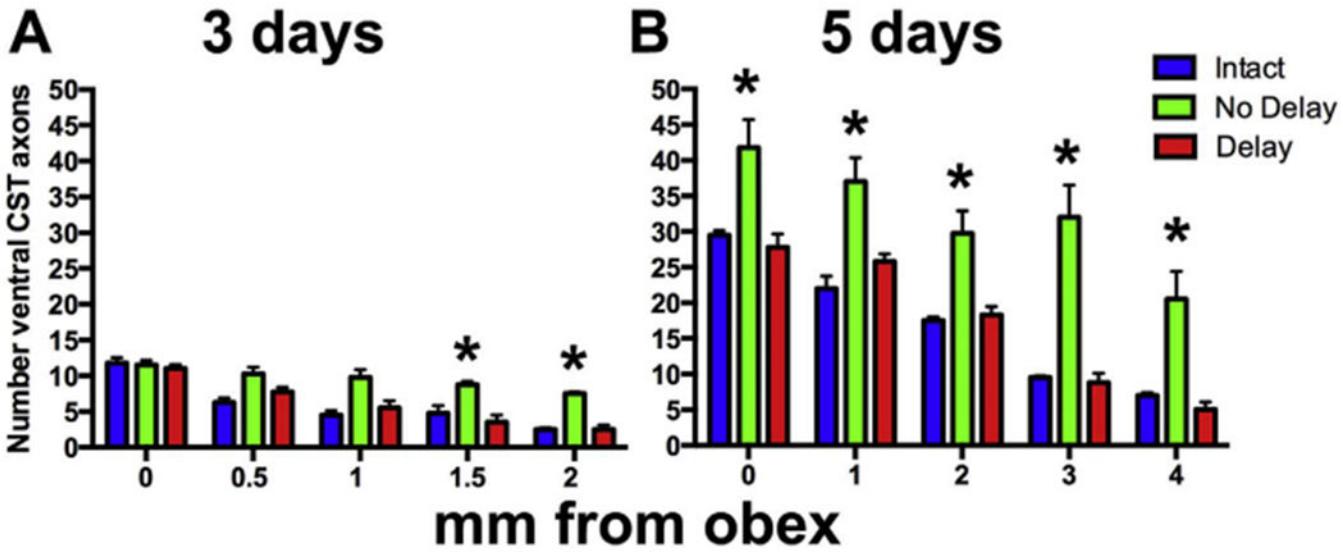

Fig. 11.

Rate of BDA transport varies by timing to lesion. (A) BDA-labeled ventral CST axons after 3 days of transport from the cortex. Intact ventral CST axons are labeled approximately 3 mm from the obex/C1 border. Among Lesion/No Delay group, ventral CST axons are labeled at least 4 mm more distally from the obex/C1 border. In the Lesion/Delay group, the distance of axonal labeling is similar to Intact animals, with axons labeled approximately 3 mm from the obex/C1 border. (B) Quantification of ventral CST axon number in transverse sections at intervals from the obex/C1 border after 5 days of transport. ANOVA among the groups at each time point reveal no significant differences in axon number at the obex/C1, but significant differences at distances beyond (ANOVA $p < 0.05$, post-hoc Fischer's $p < 0.05$ comparing Lesion/Delay group to the Intact and Lesion/No Delay groups, respectively; N = 4 rats/group). Similarly, following 5 days of transport, the number of ventral CST axons is significantly increased in the Lesion/No Delay group compared to other groups at all distances beyond the obex. With the passage of these two additional days, there total number of labeled axons has increased in all groups at all distances, indicating ongoing transport of BDA. Mean number of BDA labeled ventral CST axons + standard error (N = 4/group) are plotted in D.